Mechanism of inhibition defines CETP activity: a mathematical model for CETP in vitro

Laura K. Potter,[1,2,*] Dennis L. Sprecher,[†] Max C. Walker,[†] and Frank L. Tobin[§]

Scientific Computing and Mathematical Modeling,* GlaxoSmithKline, Research Triangle Park, NC and Cardiovascular and Urogenital Center of Excellence for Drug Discovery[†] and Scientific Computing and Mathematical Modeling,[§] GlaxoSmithKline, King of Prussia, PA

Abstract **Because cholesteryl ester transfer protein (CETP) inhibition is a potential HDL-raising therapy, interest has been raised in the mechanisms and consequences of CETP activity. To explore these mechanisms and the dynamics of CETP in vitro, a mechanistic mathematical model was developed based upon the shuttle mechanism for lipid transfer. Model parameters were estimated from eight published experimental datasets, and the resulting model captures observed dynamics of CETP in vitro. Simulations suggest the shuttle mechanism yields behaviors consistent with experimental observations. Three key findings predicted from model simulations are: *1*) net CE transfer activity from HDL to VLDL and LDL can be significantly altered by changing the balance of homoexchange versus heteroexchange of neutral lipids via CETP; *2*) lipemia-induced increases in CETP activity are more likely caused by increases in lipoprotein particle size than particle number; and *3*) the inhibition mechanisms of the CETP inhibitors torcetrapib and JTT-705 are significantly more potent than a classic competitive inhibition mechanism with the irreversible binding mechanism having the most robust response. In summary, the model provides a plausible representation of CETP activity in vitro, corroborates strong evidence for the shuttle hypothesis, and provides new insights into the consequences of CETP activity and inhibition on lipoproteins.**—Potter, L. K., D. L. Sprecher, M. C. Walker, and F. L. Tobin. **Mechanism of inhibition defines CETP activity: a mathematical model for CETP in vitro. *J. Lipid Res.* 2009.** 50: **2222–2234.**

Supplementary key words cholesteryl ester transfer protein • reverse cholesterol transport • lipoprotein metabolism • lipemia • CETP inhibitors

Cholesteryl ester transfer protein (CETP) plays a critical role in reverse cholesterol transport (1–3). CETP facilitates the net transfer of cholesterol ester (CE) from HDL to VLDL and LDL, which is followed by hepatic uptake of LDL via the LDL receptor (4). The CETP-mediated transfer of CE is part of a bidirectional exchange that also includes the transfer of triglyceride (TG) from VLDL and LDL to HDL (1–3).

The relationship between CETP and atherosclerosis/coronary heart disease (CHD) is unclear, as is the importance of the net transfer of CE from HDL to apolipoprotein (apo)B-containing lipoproteins. CETP deficiency and inhibition studies in animals and humans have produced conflicting results. Pharmacologic CETP inhibition has increased HDL cholesterol and reduced atherosclerosis in rabbit models (5). In humans, CETP deficiency has been associated with both increased and decreased CHD risk (3, 5). The CETP inhibitors JTT-705 and torcetrapib have been shown to effectively reduce CETP activity in humans and raise HDL cholesterol, although the effect of this class of compounds on atherosclerosis and CHD risk is as yet unclear (6–8).

Adding to this uncertainty is the termination of a Phase III torcetrapib study following an unexpected increase in deaths when dosed in combination with statin therapy versus statin therapy alone. "Off-target" activities of torcetrapib have been suggested as the reason for increased mortality and morbidity (9) and atherosclerotic plaque volume decreases were seen in the subset of patients having the greatest HDL changes (10). It is not yet known, however, if the increases in mortality and morbidity were caused entirely by the proposed mechanism or were in part due to changes in HDL subfractions or in functionality induced by CETP inhibition itself (11). Studies with other CETP inhibitors in development may shed light on whether this is a generalized phenomenon or specific to certain compounds, patient groups, or lipid phenotypes.

The inhibitors JTT-705 and torcetrapib block CETP activity via different mechanisms. JTT-705 irreversibly binds

Manuscript received 16 January 2009 and in revised form 4 March 2009.

Published, JLR Papers in Press, March 11, 2009
DOI 10.1194/jlr.M900015-JLR200

Abbreviations: apoB, apolipoprotein B; CETP, cholesteryl ester transfer protein; CE, cholesterol ester; CHD, coronary heart disease; LTIP, lipid transfer inhibitor protein; TG, triglyceride.

[1] Present address of L. K. Potter: Computational Biology, Syngenta Biotechnology, Inc., Research Triangle Park, NC.

[2] To whom correspondence should be addressed.
e-mail: laura.potter@syngenta.com

Copyright © 2009 by the American Society for Biochemistry and Molecular Biology, Inc.

This article is available online at http://www.jlr.org

Downloaded from www.jlr.org by guest, on June 14, 2012

to CETP and prevents CETP-lipoprotein binding (7). Torcetrapib is more potent (8) and acts as a noncompetitive inhibitor by binding reversibly to CETP where the resulting complex can bind to lipoproteins and form an inactive complex that is unable to complete transfer of lipids (7). It is unclear, however, what the consequences of different inhibition mechanisms may be on CETP transfer activity and lipoprotein metabolism in general.

Evidence suggests that both the lipid composition and the relative particle numbers of lipoproteins influence CETP activity and the net transfer of CE from HDL to apoB-containing lipoproteins (2, 12, 13). Several human studies have shown increased CE transfer and CETP activity in individuals with higher TG levels including temporary postprandial increases as well as in hyperlipidemia (13–18). When high TG levels are sustained, the increased CE transfer mediated by CETP yields higher levels of small, dense, proatherogenic LDL particles (8). This increase in CETP activity may be due to the higher levels of TG rather than increases in CETP protein (13). CE transfer activity is also augmented in hypercholesterolemia, playing a role in shifting the LDL profile toward smaller, more dense particles (19). Whether lipemia-induced increases in CETP activity result directly from heightened apoB-containing lipoprotein particle number, size, or both is unclear.

To gain better insight into the overall effect of CETP on net CE transfer and reverse cholesterol transport, it is important to understand the consequences of CETP inhibition and the relationship between CETP and lipoprotein particle number and composition. Learning more about the mechanisms and implications of CETP-mediated lipid transfer can help shed light on the complex interrelationships between HDL and the apoB-containing lipoproteins and how therapeutic modifications to the system could impact HDL and LDL mass, composition, and clearance.

Mathematical models can help dissect the complex dynamics of lipoprotein metabolism and provide a greater understanding of the role CETP plays. By comprehensively detailing the kinetics and interactions of CETP activity, a kinetic model could predict the effects of CETP inhibition and the differences in inhibitory mechanisms. A model also could explore issues related to lipoprotein particle size and composition with a view toward predicting and explaining the relative atherogenicity of a given lipoprotein particle profile. The first step in building such a model is to capture the dynamics of CETP activity in vitro, including the binding and the details of the lipid exchange processes. Such a model could be a building block in a larger model of in vivo lipoprotein metabolism to explore CETP biology and investigate inhibition of different components of lipoprotein metabolism.

In this article, a mathematical model for CETP activity in vitro is presented. The model tracks the binding and lipid transfer kinetics of CETP and lipoprotein species by class including the cholesterol and triglyceride contents of the various lipoprotein classes. Model parameters were carefully estimated via mathematical optimization by simultaneously comparing the model to multiple experimental datasets. The resulting model is able to predict the dynamics of CETP activity and inhibition on lipoprotein particles in vitro.

METHODS

Conceptual model for CETP activity

There are two prevailing hypotheses for the mechanism of CETP activity: the shuttle model and the ternary complex model (20, 21). In the shuttle model, CETP can bind to CE and TG, and accumulates "stores" of CE and TG that can be subsequently exchanged with lipoproteins. Such an exchange begins with CETP binding to a lipoprotein (**Fig. 1**, Step 1) (22) followed by the bidirectional transfer of lipids between the lipoprotein and CETP (Fig. 1, Step 2). The exchange is followed by CETP dissociation (Fig. 1, Step 3) and the CETP molecule is then free to continue binding and exchanging with additional lipoproteins.

The ternary complex model (23) postulates that CETP binds to a lipoprotein particle, which, in turn, leads to binding with another lipoprotein to form a complex of CETP bound between two lipoproteins. This is followed by the transfer of neutral lipids between the two lipoproteins, and, finally, the dissociation of the lipoprotein particles.

Experimental evidence from several studies provides strong support for the shuttle model. CETP can bind to neutral lipids (22, 24) and those lipids can be transferred back and forth between CETP and lipoproteins (25). Moreover, a recent study detailing the crystal structure of CETP suggests that CETP binds to only a single lipoprotein at a time, forming a "tunnel" with both ends bound to the lipoprotein (24). Both CE and TG can be exchanged between the CETP molecule and the bound lipoprotein by the flow of neutral lipids through the tunnel. These findings are consistent with the shuttle theory for CETP-mediated lipid transfer.

Limited kinetic models have been developed based on both the shuttle (25–27) and ternary complex (23) hypotheses. They provided reasonable approximations to CE transfer data, although none of these models were designed to describe TG transfer activity directly, and hence they are not able to capture the key exchange dynamics of CE and TG together. The detailed crystal structure of CETP (24) provides compelling evidence for the shuttle model over the ternary complex model because it appears that the CETP molecule can bind to only one lipoprotein

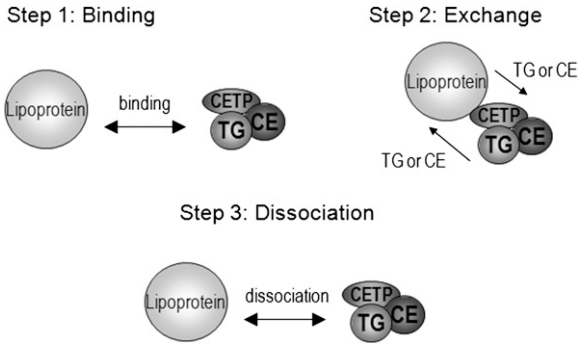

Fig. 1. Shuttle model for CETP mechanism. Based on the shuttle model, CETP associates with molecules CE and TG. CETP transfers lipid between lipoproteins by (1) binding to a single lipoprotein and (2) facilitating a homo- or hetero-exchange of neutral lipids between CETP and the lipoprotein. The exchange is followed by dissociation of CETP from the lipoprotein particle (3). Note that binding and dissociation (1) and (3) can occur without any exchange activity, effectively bypassing (2).

Downloaded from www.jlr.org by guest, on June 14, 2012

particle at a time. Therefore, in this article, we will consider only the shuttle mechanism for CETP activity. The resulting model, presented here, captures all the relevant behaviors of CETP activity, including binding, bidirectional lipid exchange of CE and TG, and dissociation.

The major assumptions used in building the shuttle-based model follow.

Equimolar exchange of lipids. Equimolar exchange occurs when the number of molecules transferred from a CETP-bound lipoprotein to CETP is equal to the number of molecules transferred back from CETP to the lipoprotein, yielding no net gain or loss of core lipids. Several experimental studies have reported equimolar CETP-mediated exchange of neutral lipids (28–31), whereas others have shown a depletion of core lipids in HDL species, particularly in the presence of unesterified fatty acids (32–35). Given the data showing equimolar exchange can occur and that monoclonal antibody evidence (28) suggests a tight coupling between CE and TG exchange, we will assume that the exchanges are equimolar, at least in the case of the in vitro environment with isolated lipoproteins and low levels of unesterified fatty acids. If necessary, this assumption can easily be relaxed to allow nonequimolar exchange.

Homoexchange and heteroexchange of lipids. Assuming equimolar exchange, there are four possible scenarios for the exchange of lipid between CETP and a bound lipoprotein: a heteroexchange of *1*) CE for TG or *2*) TG for CE, or a homoexchange of *3*) CE for CE or *4*) TG for TG. Evidence suggests a relative preference for homoexchange over heteroexchange (36). Homoexchange effectively competes with heteroexchange by tying up CETP in a nonproductive manner, blocking the net CE transfer from HDL to the apoB-containing lipoproteins.

Effects of core lipid composition on transfer activity. The relative preference for the donation of CE versus TG from a lipoprotein to CETP is a function of the relative concentrations of CE and TG in the lipoprotein's core (29). In an in vitro incubation, CETP activity will attain equilibrium when all lipoproteins in the incubation have the same CE:TG ratio (20).

A complete list of assumptions used in developing the conceptual model are detailed in Appendix I.

Mathematical model

The corresponding mathematical model is a system of ordinary differential equations that describes the rate kinetics of each process: changes in CETP binding, lipid transfer activities, and the composition of the lipoproteins. Depending on the type of in vitro experiment, the lipoproteins involved in the exchange may include two or more separate classes or subclasses (e.g., LDL, VLDL, HDL3, etc.). For each lipoprotein species, the model tracks the "average" lipoprotein particles of each class, as well as their corresponding TG and CE compositions. These concentrations are further distinguished by the lipoproteins that are bound and unbound to CETP. Finally, the model also includes the concentrations of CETP and the CE and TG associated with the CETP particles.

The model includes the simultaneous binding and exchange between CETP and the different lipoprotein species as individual lipoproteins bind to CETP molecules, exchange lipids, and dissociate. For example, consider the in vitro incubation of LDL, VLDL, and lipoprotein-free plasma (a source of CETP) for 18 h, as described in (37) and Experiment 1 of **Table 1**. In this case, the following simultaneous activities are modeled:

Binding:

$$\text{CETP} + \text{LDL} \rightarrow \text{CETP•LDL complex}$$
$$\text{CETP} + \text{VLDL} \rightarrow \text{CETP•VLDL complex}$$

Lipid exchange:

CE/TG exchange between CETP and LDL in the CETP • LDL complex
CE/TG exchange between CETP and VLDL in the CETP • VLDL complex

Dissociation:

$$\text{CETP} \bullet \text{LDL} \rightarrow \text{CETP} + \text{LDL}$$
$$\text{CETP} \bullet \text{VLDL} \rightarrow \text{CETP} + \text{VLDL}$$

In effect, the different lipoprotein species are competing for free CETP in order to bind with it and perform a lipid exchange. The result is a network of interacting particles that affect CE and TG exchange between the different lipoproteins, with CETP acting as the intermediary transfer agent.

Depending on the in vitro experiment being considered, the general CETP model is customized to consider only those lipoprotein species involved. The resulting model is a system of $6n+3$ differential equations, where n is the number of distinct lipoprotein species. For example, in the case of Experiment 1 described above and in Table 1, there are two lipoprotein species and 15 differential equations. The model variables are described in **Table 2**. There are seven parameters in the model (**Table 3**), together with additional experiment-specific param-

TABLE 1. Experimental data used in model calibration

Exper.	Incubation	Measurement	Reference
1	VLDL, LDL, LFP for 18 h	LDL TG:CE ratio over time	(37)
2	VLDL, LDL, LFP for 18 h	Final weight ratios of CE and TG in VLDL and LDL	(37)
3	VLDL, LDL, LFP for 18 h	Final LDL TG:CE ratio with respect to different initial VLDL:LDL protein ratios	(37)
4	VLDL, HDL2, LFP for 18 h	Final HDL2 TG:CE ratio with respect to different initial VLDL-TG:HDL2-CE ratios	(40)
5	VLDL, HDL3, LFP for 18 h	Final HDL3 TG:CE ratio with respect to different initial VLDL-TG:HDL3-CE ratios	(40)
6	VLDL, LDL, HDL, PP-CETP for 24 h	Final amounts of CE in LDL and HDL	(36)
7	LDL, CE- and TG-labeled HDL3, CETP for 2 h	Percent of label transferred from HDL3 to LDL over time	(25)
8	LDL, CE- and TG-labeled HDL3, CETP for 2 h	Final percent of label transferred from HDL3 to LDL with respect to amount of CETP	(25)

LFP denotes lipoprotein-free plasma, a source of unpurified CETP; PP-CETP denotes partially purified CETP.

Downloaded from www.jlr.org by guest, on June 14, 2012

TABLE 2. Model variables

Model Variable	Symbol
Free (unbound) lipoprotein particle of species *j*	LP_j^f
CE in free lipoproteins of species *j*	$CE_{LP_j^f}$
TG in free lipoproteins of species *j*	$TG_{LP_j^f}$
Lipoprotein particle of species *j* bound to CETP	LP_jC
CE in lipoproteins of species *j* bound to CETP	CE_{LP_jC}
TG in free lipoproteins of species *j* bound to CETP	TG_{LP_jC}
Free CETP particles	$CETP^f$
CE associated with CETP	CE_{CETP}
TG associated with CETP	TG_{CETP}

The model variables represent lipoprotein particles, CETP particles, and the corresponding CE and TG in those particles. The total number of variables is $6n+3$, where n is the number of distinct lipoprotein species in the incubation (e.g., LDL, HDL3, etc.). Amounts are given in μmols and concentrations are in μM.

eters (**Table 4**) that represent any unspecified conditions such as the initial amount of CETP in the incubation. The model equations are given in Appendix II together with a detailed derivation.

Model implementation and calibration

The model was implemented computationally in Matlab (The Mathworks, Natick, MA). A numerically robust stiff ordinary differential equation solver (38) with tight tolerances was used to compute numerical solutions. This particular solver is designed to handle systems where the dynamics of one or more variables may occur on a different time scale than the others. This is a potential issue for the CETP model because the time scales of binding and lipid transfer may be significantly different.

The model parameters can be classified into two categories: base model parameters and experiment-specific parameters. The base parameters apply to all model simulations and are given in Table 3. The experiment-specific parameters are unique to each experiment and have been added to account for key information that has not been measured or supplied, such as the amount of CETP added to the incubation or the initial CE:TG ratio in the lipoproteins at the start of the experiment (Table 4). This increases the number of parameters to be determined from the data, making the fitting process itself more complex. However, this inclusion is necessary to make sure that the base model parameters are consistently representing CETP biology only, not explaining the experimental nuances of each dataset.

Model parameters were estimated by comparing eight different experimental datasets with model simulations corresponding to the respective experiment. The estimation process involved least squares optimization techniques (39) to simultaneously fit the model against eight different published datasets so that one set of base model parameters could explain all data. The experimental data are from in vitro incubations of lipoproteins with CETP and the measurements include lipoprotein TG:CE core lipid ratios and CE and TG mass transfers over time or with respect to CETP or lipoprotein levels (25, 36, 37, 40). See Table 1 for details on each of the eight experiments.

Because these data are from different experiments with different experimental conditions, they will have varying levels of noise and possible inconsistencies. However, the assumption is made that, together, they provide key information about kinetic behaviors of many different CETP components in the system. In a sense, the process of fitting all the data simultaneously acts as an "averaging" strategy to take into account any small differences in the manner in which the assays are conducted. The result is a single parameter set that incorporates all the available dynamics of the system in a consistent manner across all eight experiments. The quality of each of the fits is evidence that this strategy appears to be successful.

Details of the model calibration process are given in Appendix III.

RESULTS

Model calibration

The estimated base and experiment-specific model parameters are given in Table 3 and Table 4, respectively, and comparisons of the experimental data and corresponding model simulations are depicted in **Figs. 2–4**. As seen in the figures, the model reasonably captures the dynamics of CETP-mediated lipid transfer between lipoproteins in vitro. These dynamics include time course behavior, as in Figs. 2, 4A, and 4B, as well as changes in response to varying initial amounts of lipoproteins and CETP, as in Figs. 3, 4C, and 4D. Moreover, the model re-

TABLE 3. Base model parameters

Parameter	Symbol	Value	Reference
Volume of incubation	V	Experiment-dependent	NA
Association rate for lipoprotein:CETP	k_{on}	10 $uM^{-1}min^{-1}$	(45)
Dissociation rate for lipoprotein:CETP	k_{off}	2.2 min^{-1}	Estimated
Lipid transfer rate	k_{tr}	$1.0x10^{-13}$ min^{-1}	Estimated
Relative preference for homo-exchange vs. hetero-exchange	α	0.62	Estimated
Initial amount of CE (and TG) associated with CETP	CE_{CETP0}	2.44 molcules	Estimated
Relative inhibition of LDL-CETP transfer activity by LTIP	k_{LDL}^{LTIP}	0.73	Estimated

The parameters listed apply to all experiments, whereas the experiment-specific parameters are given in Table 4. Estimated parameters were determined according to the algorithm given in Model Development.

Downloaded from www.jlr.org by guest, on June 14, 2012

TABLE 4 Experiment-specific parameters

Parameter	Exper.	Value
Amount of CETP in incubation	1	$1.15x10^{-5}$ umoles
Initial TG:CE weight ratio of LDL	1	0.21
Amount of CETP in incubation	2	$7.89x10^{-6}$ umoles
Amount of CETP in incubation	3	$8.12x10^{-6}$ umoles
Initial TG:CE weight ratio of LDL	3	0.08
Initial TG:CE weight ratio of VLDL	3	3.00
Amount of CETP in incubation	4,5	$3.96x10^{-5}$ umoles
Initial TG:CE weight ratio of HDL2	4	0.28
Initial TG:CE weight ratio of VLDL	4	8.00
Initial TG:CE weight ratio of HDL3	5	0.25
Initial TG:CE weight ratio of VLDL	5	8.00
Initial TG:CE weight ratio of LDL	6	0.095
Initial TG:CE weight ratio of HDL	6	0.10
Initial TG:CE weight ratio of VLDL	6	7.57
Initial TG:CE weight ratio of HDL3	7,8	0.25
Initial TG:CE weight ratio of LDL	7,8	0.13
Initial HDL3 cholesterol	7,8	0.31 umoles
Amount of CETP in incubation	7,8	$2.3x10^{-5}$ umoles
Initial LDL cholesterol	7,8	0.23 umoles

Parameters were estimated according to the algorithm given in Model Development. The experiment column indicates the experiment(s) from Table 1 to which each parameter applies.

produces the kinetics of net mass transfer using unlabeled lipoproteins (Figs. 2, 3) and the kinetics of radiolabeled lipid transfer (Fig. 4).

Correlation coefficients between the model and data for each experiment are given in the legends for Figs. 2–4, and range between 0.918 and 0.999 with an overall correlation coefficient of 0.999 for all model simulations compared with all data. These results suggest that the shuttle model can capture experimentally observed behaviors of CETP in vitro.

Sensitivity of model parameters

The sensitivity of the model response with respect to the base model parameters in Table 3 was explored using simulations corresponding to each of the eight experiments given in Table 1. Each of the base model parameters was varied one at a time by ±25%, with all other parameters held fixed at the values in Tables 3 and 4. The corresponding model simulations were then compared with the baseline values obtained with the default parameter values in Table 3.

The predicted sensitivity of the parameters was similar for all eight experiments. **Figure 5** depicts the results for Experiment 1, which, in this case, is the percent change in the final LDL TG:CE ratio with respect to changes in the model parameters. As seen in the figure, changes in the relative preference α for homoexchange versus heteroexchange have the greatest overall impact on the model response, whereas the initial amount of CE and TG associated with CETP has almost no effect. Across all experiments, the model is most sensitive to α, followed by the CETP dissociation rate k_{off}, with negligible sensitivity to the initial amount of CE and TG associated with CETP.

Predicted effects of lipoprotein particle size and number on CETP activity

The CETP model was used to explore in vitro CETP activity under varying conditions of increased particle size and particle number, singly and in combination. Looking at this issue with Experiment 7 (as detailed in Table 1), the initial concentrations of LDL particles, LDL CE, and TG were varied to simulate changes in particle number and size. These initial concentrations were varied to range from 0.01 to 100 times the concentrations used in the actual experiment.

First, the effects of particle size and number were explored separately, where LDL particle size was varied in one simulation and LDL particle number was varied in a second simulation. **Figs. 6A** and B depict the predicted transfer of labeled CE from HDL3 to LDL after 2 h incubation with CETP for these two cases:

Varying LDL particle size, constant particle number (Fig. 6A). As particle size increases, more lipid is available for exchange with CETP, facilitating increased CE transfer from HDL3 to LDL.

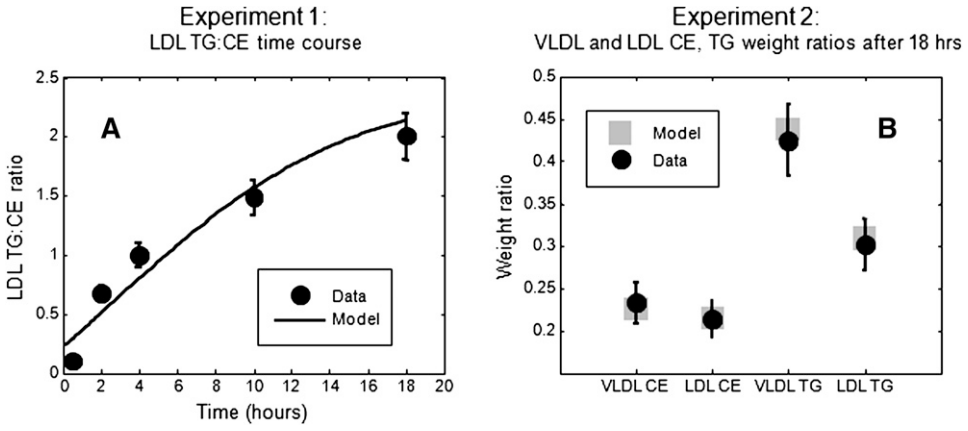

Fig. 2. Comparison of data and model fits for Experiments 1 and 2. Details of the in vitro experiments are given in Table 1, and a description of the parameter estimation process is given in Model Development. A: Time course of the LDL TG:CE ratio during incubation of LDL, VLDL, and lipoprotein-free plasma. B: Final weight ratios of CE and TG in VLDL and LDL after 18 h incubation of LDL, VLDL, and lipoprotein-free plasma. Correlation coefficients between the model and data for each experiment: (A) 0.974, (B) 0.999.

Downloaded from www.jlr.org by guest, on June 14, 2012

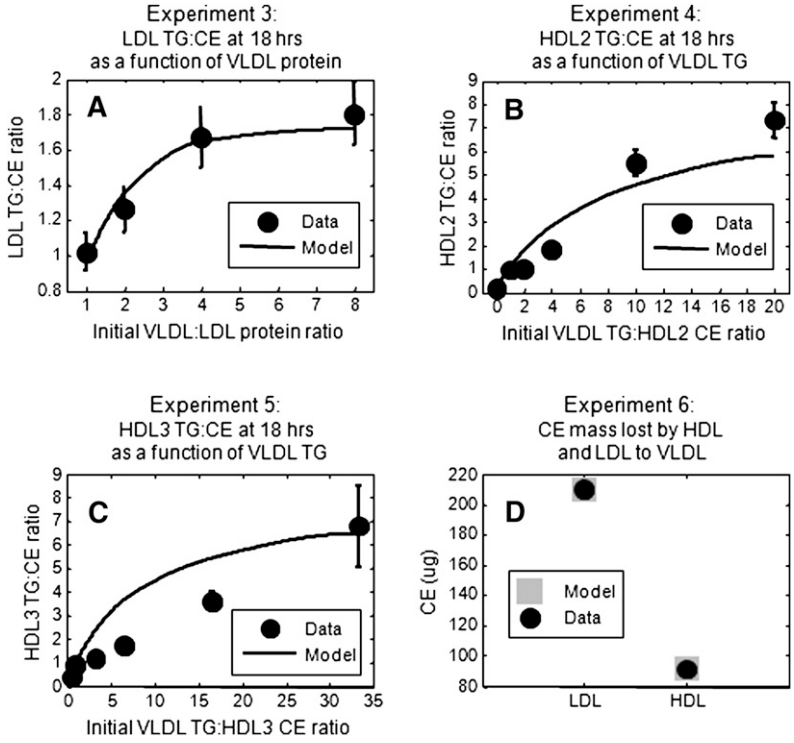

Fig. 3. Comparison of data and model fits for Experiments 3–6. Details of the in vitro experiments are given in Table 1, and a description of the parameter estimation process is given in Model Development. A: Final ratio of TG:CE in LDL after 18 h incubation of VLDL, LDL, and lipoprotein-free plasma, where the initial VLDL:LDL protein ratio was varied. B: Final ratio of TG:CE in HDL2 after 18 h incubation of VLDL, HDL2, and lipoprotein-free plasma, where the initial VLDL-TG:HDL2-CE ratio was varied. C: Final ratio of TG:CE in HDL3 after 18 h incubation of VLDL, HDL3, and lipoprotein-free plasma, where the initial VLDL-TG:HDL3-CE ratio was varied. D: Final CE mass in LDL and HDL following incubation of LDL, HDL, VLDL, and partially purified CETP for 24 h. Correlation coefficients between the model and data for each experiment: (A) 0.978, (B) 0.973, (C) 0.918, (D) Not enough data.

Varying LDL particle number, constant size (Fig. 6B). The CE transfer from HDL3 to LDL has a U-shaped response, with lower levels of transfer for both low and high numbers of LDL particles. The decreased transfer results from a greater relative abundance of HDL3 or LDL, which effectively blocks net CE transfer. The transfer is maximal when the relative particle numbers are balanced so that both interact with CETP at sufficient levels.

Because lipemia often involves the increase of both particle size and number simultaneously, the model was used to predict the effects of varying size and number together. Three separate simulations are given in Fig. 6C, where particle size and number were varied according to the following scenarios: *a*) more abundant small particles: size increases by 1/10th of the increase in particle number; *b*) more abundant particles of the original size: particle size and number increases are identical; and *c*) more abundant large particles: size increases by 10 times the increase in particle number.

As seen in Fig. 6C, the net CE transfer increases with particle number until the LDL particles become too abundant and effectively block CE transfer from HDL.

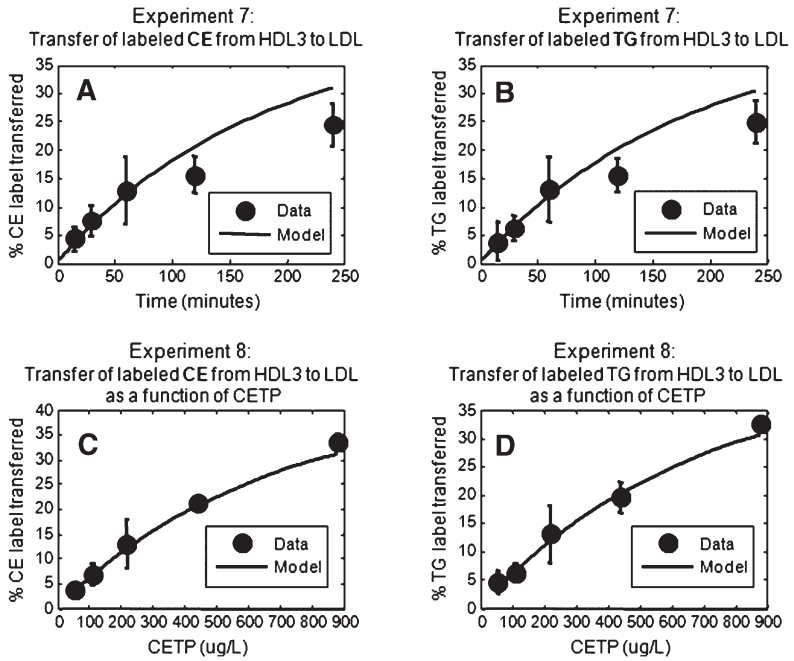

Fig. 4. Comparison of data and model fits for Experiments 7 and 8. Details of the in vitro experiments are given in Table 1, and a description of the parameter estimation process is given in Model Development. A, B: Time course of percentage of labeled CE (A) and TG (B) transferred from HDL3 to LDL during incubation with CETP. C, D: Percentage of labeled CE (C) and TG (D) transferred from HDL3 to LDL after 2 h incubation with varying initial concentrations of CETP. Correlation coefficients between the model and data: (A) 0.988, (B) 0.985, (C) 0.993, (D) 0.996.

Downloaded from www.jlr.org by guest, on June 14, 2012

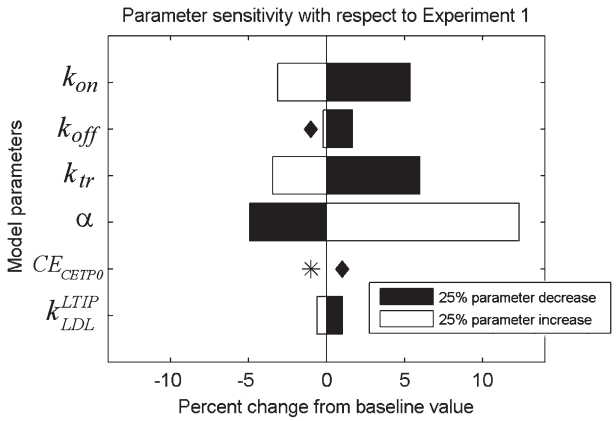

Fig. 5. Sensitivity of model parameters. Each base model parameter (see Table 3) was varied by ±25% and the model response corresponding to Experiment 1 (see Table 1) was computed. The graph depicts the percent change in the final LDL TG:CE ratio from the baseline value calculated with the parameter values in Table 3. The symbols ♦ and * denote percent change values less than 0.5% for the corresponding parameters that were increased/decreased (respectively) by 25%.

The net transfer is greatest for scenario (*c*), where the LDL particles are relatively larger and have more lipid to exchange.

Comparison of different mechanisms for CETP inhibition

The model was used to compare the effects of different CETP inhibition mechanisms on CETP activity. The mechanisms of the inhibitors torcetrapib and JTT-705 were compared with a classic competitive inhibitor mechanism. Simulations of CETP inhibition used the conditions corresponding to Experiment 7, which involves the incubation of CE- and TG-labeled HDL3 with LDL and CETP (see Table 1). The following CETP inhibition mechanisms were compared with the baseline conditions: *1*) competitive inhibition: inhibitor reversibly binding to CETP; *2*) noncompetitive inhibition (torcetrapib mechanism): inhibitor binding reversibly to CETP, with subsequent reversible binding to lipoproteins to form a complex incapable of lipid transfer; and *3*) irreversible binding of inhibitor to CETP (JTT-705 mechanism).

Predictions were conducted with varying inhibitor concentrations or inhibitor binding affinities to explore the effects of inhibitor affinity and concentration on CETP activity. All dissociation rates for the inhibitor were assumed to be equal to the CETP-lipoprotein dissociation rate, and the inhibitor concentration and binding association rate were set to the corresponding values for CETP when they were not varied in the simulation.

As seen in **Fig. 7**, the model predicts that noncompetitive and irreversibly binding CETP inhibitors are considerably more potent at blocking CE transfer activity than an inhibitor with a classic competitive inhibition mechanism, which had relatively little effectiveness. Increasing the relative binding affinity of the inhibitor greatly improves the level of CETP inhibition except in the case of the competitive inhibitor, which achieves only slight improvement as the affinity increases (Fig. 7A). The same effect is seen when inhibitor concentration is increased while the affinities are held constant (Fig. 7B). Under the conditions of these in vitro simulations, the irreversible binding inhibitor appeared to be most potent at blocking CE transfer activity.

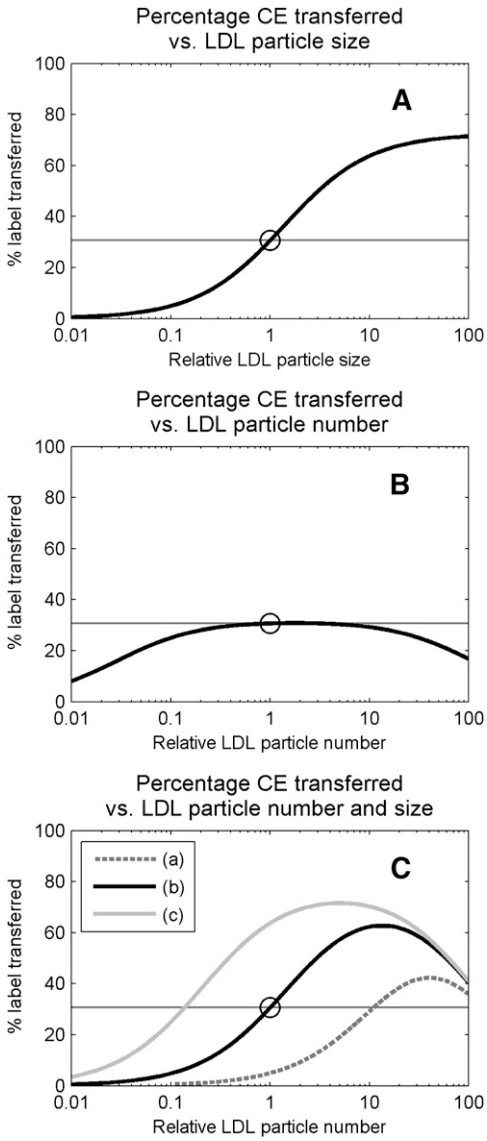

Fig. 6. Computational experiment comparing effects of varying LDL particle size and/or number. Model simulations corresponding to Experiment 7 in Table 1 were generated with varying initial concentrations of LDL particles and LDL lipids. A: Initial LDL particle size was varied by holding the particle number constant while varying the initial amounts of TG and CE. B: Initial LDL particle number was varied while the size was held constant by fixing the initial amounts of TG and CE. C: Initial LDL particle number and size were varied according to the following: (a) size increase is 1/10th the increase in particle number; (b) particle size and number increases are identical; (c) size increase is 10 times the increase in particle number. Each graph shows the predicted percentage of labeled CE transferred from HDL3 to LDL after four h of incubation with CETP. The thin gray line and the open circle represent the percent label transferred from the actual experiment.

Downloaded from www.jlr.org by guest, on June 14, 2012

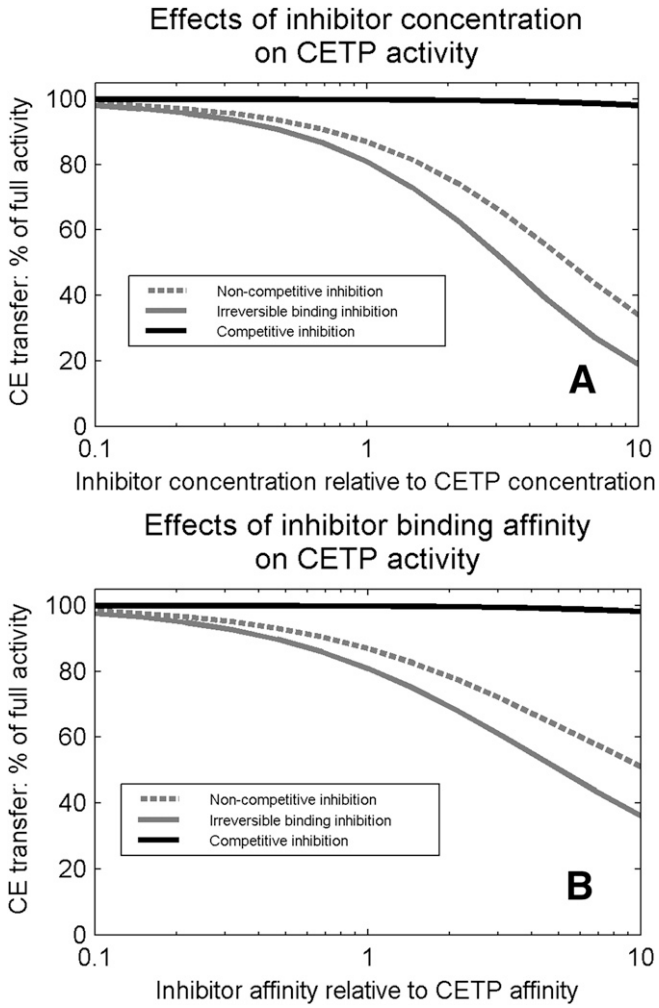

Fig. 7. Comparison of mechanisms for CETP inhibition. Model predictions corresponding to Experiment 7 in Table 1 were conducted, with simulations of CETP inhibition by three different mechanisms. Competitive inhibition involves reversible binding of inhibitor to CETP. The noncompetitive inhibition mechanism represents reversible binding of inhibitor to CETP and subsequent reversible binding of the CETP-inhibitor complex to lipoproteins, forming an inactive complex that is unable to complete lipid transfer. The irreversible binding mechanism corresponds to irreversible binding of inhibitor to CETP. The graphs represent the percentage of CE transfer that occurs in the presence of inhibitor compared with the full activity in the baseline simulation, where (A) inhibitor concentration is varied relative to CETP concentration, and (B) inhibitor binding affinity is varied relative to CETP affinity.

DISCUSSION

Employing the shuttle mechanism for lipid transfer, the mathematical model presented here is able to reproduce both dynamic and dose-dependent behaviors seen in published experimental data. These results indicate that the kinetics of the shuttle mechanism can produce behavior consistent with CETP activity in vitro, corroborating the strong experimental evidence supporting the shuttle model. Note that this does not rule out the plausibility of the ternary complex conceptual model, although a recent finding based on CETP's crystal structure indicates that CETP appears to be unable to bind more than one lipoprotein simultaneously (24). A future study could consider the ternary complex conceptual model to further evaluate its plausibility in comparison to the shuttle-based model developed here.

A key finding of the model is that the net transfer activity of CETP is strongly influenced by the relative preference for homoexchange versus heteroexchange of lipids. The model corroborates experimental evidence (36), suggesting that homoexchange occurs more frequently than heteroexchange so that net CE transfer from HDL to apoB-containing lipoproteins is effectively inhibited by the nonproductive homoexchange activity. This may be related to the physical structure of the CETP tunnel, (24) which appears to allow the passage of CE molecules more easily than the larger TG. Based on the model predictions, modulating CETP to alter this relative preference could significantly change net CE transfer activity. If possible, such a modulation could yield a new class of CETP inhibitor by effectively decreasing the productive heteroexchange activity. One potential avenue for reducing heteroexchange is to block TG transfer while preserving CE transfer, which has been achieved experimentally with the CETP monoclonal antibody LT-J1 (41).

Model simulations also suggest that lipemia affects CETP transfer activity differently depending on whether the lipemia results from increased lipoprotein particle size or number. As seen in Fig. 6A, increases in particle size (via core lipid content) yield increased CE transfer, eventually attaining a maximal level of transfer. In contrast, increases in lipoprotein particle number can either improve or reduce CE transfer activity (Fig. 6B) depending on the number of particles relative to the other lipoproteins. If the concentration of one species significantly outnumbers the other species, the dominant species can tie up more CETP and effectively inhibit the transfer of CE from HDL to apoB-containing lipoproteins. This effect is seen even when increases in particle number are concurrently accompanied by increases in particle size (Fig. 6C) although the larger particles have a greater capacity to facilitate net transfer.

These predictions suggest that increased CE transfer activity observed in postprandial and chronic lipemia are more directly related to increased lipid core content rather than an increase in particle numbers, although both can have a positive effect under the right conditions. It is not clear if changes in lipoprotein particle numbers in vivo are dramatic enough to significantly alter net CETP transfer by overwhelming available CETP with a single type of lipoprotein. Moreover, any lipemia-induced increase in particle number is typically accompanied by larger particle size in cases such as postprandial lipemia, hypercholesterolemia, and hypertriglyceridemia. Further experimental studies could help shed light on the relationship between lipoprotein particle size and number and the resulting effects on CE transfer activity, which could improve our understanding of the implications of lipemia on lipoprotein metabolism.

By exploring the effects of CETP inhibition, the predictions suggest that the mechanisms of the CETP inhibitors JTT-705 and torcetrapib (irreversible binding and non-

Downloaded from www.jlr.org by guest, on June 14, 2012

competitive mechanisms, respectively) are significantly more potent at blocking CETP activity than a competitive inhibitor. Under the assumption that all inhibitor binding affinities and concentrations are equal, the most effective mechanism is the irreversible binding inhibitor. This suggests that if specificity in targeting CETP is established, this mechanism could provide the most robust increases in effectiveness when incrementally increasing the inhibitor's affinity for CETP. The fact that torcetrapib appears to be more potent in experimental studies (8) suggests it has a higher affinity for CETP than JTT-705.

As with any mathematical model of a biological system, there is inherent uncertainty in whether the model accurately reflects the biology. In many cases, there is incomplete knowledge of key biological details so that the model represents a hypothesis about the underlying mechanisms. Moreover, the ability to estimate accurate parameters depends greatly on the quality and quantity of the relevant experimental data. Our approach is to build a biologically plausible model that matches well with as much available experimental data as possible. The calibrated model then can be used to make predictions and test hypotheses, which in turn should be tested and validated experimentally.

The model calibration strategy that we applied yields a good match overall between model simulations and observed experimental behavior given the quality of the data. The fits for Experiments 4 and 5, which involve exchange between VLDL and HDL, are, however, less accurate than the fits for the other experiments. There can be several interpretations of these particular results, including model error and insufficient data. A serious and fundamental limitation is that in the absence of time course data for the VLDL-HDL exchange, it is very unlikely that the parameters of any model can adequately take into account the important time-dependent dynamics of lipid exchange for this scenario. Such is the situation we face here and it is possibly the explanation for the less-than-desirable fitting quality. One outcome of this observation is the need for new experiments with accurate temporal measurements of the VLDL-HDL exchange so that the explicit kinetics of CETP can be validated and the model parameters improved. The additional data would also help explain whether the relatively poor fits are related to errors in the model or a lack of relevant data.

It is important to note that our calibration method is just one of several valid approaches. Another technique is to fit each dataset separately and compare the resulting parameter estimates from each fit. Based on characteristics of the CETP model and the available data, we chose to fit all data simultaneously to achieve one consistent set of parameters that could explain all data. Using multiple experiments together exposes the optimization to a more complete range of kinetic behaviors, providing a better sense of closeness between the model and all experiments. The result is a more reliable and robust set of parameters that explains a much more diverse set of CETP-related phenomena than could have been obtained by fitting one experiment at a time.

Moreover, our approach also mitigates serious problems with ill-posedness (i.e., computational ambiguity) that would occur when fitting each experiment separately because there would be many more unknown parameters than data points in this particular case. As seen in Figs. 2–4, the resulting parameter set from the simultaneous fit consistently captures the known behaviors in the system as represented by the available experimental data.

By combining multiple datasets, we can partially compensate for less than optimal data such as the lack of VLDL-HDL temporal data. In the event that more comprehensive, fully temporal datasets are generated with sufficient numbers of data points in each set, it would then be feasible to fit each dataset separately as one way to understand the detailed kinetics better. This also would allow for a comparison between the two estimation approaches and the resulting parameter sets.

One major limitation of the model itself is that it may provide a relatively poor approximation to the in vivo scenario, which is also frequently the case with in vitro experimental models. The in vivo dynamics of CETP are intertwined with the activities of LCAT, lipases, receptor uptake of cholesterol in the liver, dietary uptake, cholesterol efflux, and other factors that influence lipoprotein composition and function, none of which are accounted for in an isolated in vitro setting. Therefore, neither the experimental nor mathematical in vitro models can predict the full consequences of CETP activity and inhibition in vivo. The in vitro models, however, do provide a good starting point for understanding the basic mechanisms and behaviors that are difficult to ascertain in vivo. The next logical modeling step would be to incorporate this CETP in vitro mathematical model into a larger in vivo model that accounts for the interactions between CETP and other key activities.

Even with these limitations, the CETP in vitro model can explore the dynamics of lipid transfer activity and shed light on behaviors that are difficult to measure simultaneously and exhaustively such as the net transfer activity between any two lipoprotein species and the degree of homoexchange versus heteroexchange. Moreover, these phenomena can be investigated computationally under a variety of conditions to predict the impacts of lipemia, CETP inhibition, disease, and therapeutic intervention. Insights gained from the model can help motivate and design new in vitro and in vivo experiments to better understand the implications of CETP activity and inhibition.

APPENDIX I: MODEL ASSUMPTIONS

The kinetic model for CETP activity in vitro is based on the following assumptions:

1. CETP associates directly with CE and TG molecules that in turn, can be exchanged with lipoproteins (24, 25). Recent details of CETP's crystal structure show that neutral lipids inhabit the tunnel of the CETP molecule and that these lipids are able to move back and forth between the inside of the tunnel and a lipoprotein bound to CETP (24).

Downloaded from www.jlr.org by guest, on June 14, 2012

2. CETP can bind reversibly to only a single lipoprotein particle at a time. This is based on evidence from the crystal structure of CETP (24) and that it has been shown to bind to HDL, VLDL, and LDL particles (42).

3. All lipoprotein particles have effectively the same affinity for CETP binding (42). This assumption can be relaxed if necessary. Unless there are good kinetic studies to justify the relaxation, it will be impossible to distinguish the binding affinity constants.

4. Once CETP is bound to a lipoprotein, an equimolar exchange of neutral lipids may occur between the lipoprotein and CETP (29) or CETP may dissociate without facilitating exchange. This too can be relaxed if there are sufficient quantitative experimental data to justify and calibrate the nonequimolar exchange activity.

5. This exchange of lipids between CETP and a bound lipoprotein may involve a heteroexchange of CE for TG (or TG for CE), or a homoexchange of CE for CE or TG for TG. Evidence suggests a relative preference for homoexchange over heteroexchange (36). In most cases, homoexchange can be ignored because there is no change in the lipid composition of the bound lipoprotein or CETP. Note that homoexchange must be considered when labeled lipids are used in the incubation because a homoexchange may involve trading a labeled CE for an unlabeled CE, for example. In this case, homoexchanges impact the distribution of lipids in terms of transferring label.

6. The relative preference for donation of CE versus TG is based on the relative concentrations of both CE and TG in the lipoprotein's lipid core (29).

7. Lipid transfer inhibitor protein (LTIP), or apolipoprotein F (43), inhibits lipid transfer activity between CETP and LDL, with negligible direct effects on other lipoprotein species (36). Following the lipid exchange, CETP dissociates from the lipoprotein. Note that because CETP binds reversibly to a lipoprotein, it is not required that an exchange occurs before dissociation.

8. Equilibrium of the active exchange process in each lipoprotein class is attained when all lipoproteins have equal TG:CE ratios (20).

9. The incubations are rapidly well mixed, so that any spatial variation in concentrations can be ignored.

APPENDIX II: MODEL DERIVATION

The model equations are derived using the eight assumptions given in the Model Development section, together with mass action kinetics, modified as necessary. In the experiments listed in Table 1, Experiment 6 has three lipoprotein species and all other experiments have two. The equations are presented assuming n distinct lipoprotein species, such as HDL, VLDL, etc.. The number of species will vary with the conditions of the in vitro incubation that is to be simulated.

Notation: square brackets denote concentrations, whereas variables without brackets correspond to amounts. Detailed descriptions of the model variables and parameters are given in Tables 2, 3 and 4. All concentrations are given in μM, amounts in μmoles, and time is expressed in minutes so that fluxes are given in μM/min and μmoles/min.

As suggested by the crystal structure of CETP (24), we assume that each CETP molecule can bind only to one lipoprotein particle at a time. CETP binding to lipoprotein particles is modeled using standard binding kinetics:

$$LP_j^f + CETP^f \Leftrightarrow LP_jC$$

where LP_j^f is unbound lipoprotein of species j, $CETP^f$ is unbound CETP, and LP_jC is the complex formed by binding of LP_j^f and $CETP^f$. These binding association and dissociation kinetics are represented by the following equations:

$$\frac{d\left[LP_j^f\right]}{dt} = -k_{on}\left[LP_j^f\right]\left[CETP^f\right] + k_{off}\left[LP_jC\right] \qquad (Eq.\ A1)$$

$$\frac{d\left[CETP^f\right]}{dt} = \sum_{j=1}^{n} -k_{on}\left[LP_j^f\right]\left[CETP^f\right] + k_{off}\left[LP_jC\right] \qquad (Eq.\ A2)$$

$$\frac{d\left[LP_jC\right]}{dt} = k_{on}\left[LP_j^f\right]\left[CETP^f\right] - k_{off}\left[LP_jC\right] \qquad (Eq.\ A3)$$

for j = 1,…,n, where n is the number of distinct lipoprotein species.

As the lipoprotein particles bind and dissociate from CETP, their lipid contents concurrently become available or unavailable for exchange with CETP. Therefore, the kinetics of TG and CE in unbound lipoproteins LP_j^f are given by

$$\frac{d\left[CE_{LP_j^f}\right]}{dt} = -k_{on}\left[CE_{LP_j^f}\right]\left[CETP^f\right] + k_{off}\left[CE_{LP_jC}\right] \qquad (Eq.\ A4)$$

$$\frac{d\left[TG_{LP_j^f}\right]}{dt} = -k_{on}\left[TG_{LP_j^f}\right]\left[CETP^f\right] + k_{off}\left[TG_{LP_jC}\right] \qquad (Eq.\ A5)$$

for j = 1,…,n.

The equations for the TG and CE in CETP and in lipoproteins bound to CETP include the binding-related kinetics in Eq. A1 and A2 and the dynamics of lipid transfer, which are derived next.

The exchange of lipids between CETP and a bound lipoprotein can be represented as one of four cases: *A*) homoexchange of CE for CE, *B*) homoexchange of TG for TG, *C*) heteroexchange of CE for TG, and *D*) heteroexchange of TG for CE. In each case, equimolar exchange (Assumption 4) dictates that the flux of lipid out of the lipoprotein is equal to the flux of lipid coming into the lipoprotein. Moreover, Assumption 6 implies that the rate of CE leaving the lipoprotein is proportional to the relative amount of CE versus TG in the core and a similar relation applies to the rate of TG

Downloaded from www.jlr.org by guest, on June 14, 2012

leaving the particle. Because the flux of CE and TG depends on their relative concentrations in both the donor and acceptor particle, both relative concentrations are included in the flux in a multiplicative manner, which is a simple and standard way to incorporate the effects of two interacting species. Thus, for Case (*A*), we have the following expression for lipid exchange between a single molecule of CETP bound to a lipoprotein particle of the jth species:

$$\text{Flux of CE leaving } LP_jC \text{ molecule} = \text{Flux of CE entering } LP_jC \text{ molecule}$$
$$= k_{tr}k_i^{LTIP}\alpha\left(\frac{CE_{LP_jC}}{CE_{LP_jC}+TG_{LP_jC}}\right)\left(\frac{CE_{CETP}}{CE_{CETP}+TG_{CETP}}\right) \quad (Eq.\ A6)$$

for j = 1,…,n. The constant α represents the relative preference for homoexchange of lipids versus heteroexchange, reflecting the effective competition between the two types of exchange activity.

The overall flux rate of CE homoexchange between lipoproteins of species j bound to CETP is given by the flux rate in Eq. A6 multiplied by the number of LP_j:CETP complexes:

$$\text{Flux of CE leaving } LP_jC = \text{Flux of CE entering } LP_jC$$
$$=10^{-6}N_0k_{tr}k_j^{LTIP}\alpha LP_jC\left(\frac{CE_{LP_jC}}{CE_{LP_jC}+TG_{LP_jC}}\right)\left(\frac{CE_{CETP}}{CE_{CETP}+TG_{CETP}}\right) \quad (Eq.\ A7)$$

for j = 1,…,n.

where N_0 represents Avogadro's number. Note that since the flux rate in Eq. A7 depends on the amount of lipoprotein:CETP complex, there is no transfer in the absence of CETP-lipoprotein binding. The rate also depends on the relative amount of CE versus TG in the lipoprotein, reflecting that lipids are competing for interaction with CETP as in Assumption 6. Finally, the dependence on the concentration of CE associated with CETP indicates that the bidirectional homoexchange of CE for CE is dependent on the levels of CE in both donor and acceptor particles.

A similar rate expression applies for the homoexchange of TG for TG as in Case (*B*):

$$\text{Flux of TG leaving } LP_jC = \text{Flux of TG entering } LP_jC$$
$$=10^{-6}N_0k_{tr}k_j^{LTIP}\alpha LP_jC\left(\frac{TG_{LP_jC}}{CE_{LP_jC}+TG_{LP_jC}}\right)\left(\frac{TG_{CETP}}{CE_{CETP}+TG_{CETP}}\right) \quad (Eq.\ A8)$$

for j = 1,…,n

For the heteroexchange cases (*C*) and (*D*), the rate expressions are given by

$$\text{CE flux out of } LP_jC = \text{TG flux into } LP_jC$$
$$=10^{-6}N_0k_{tr}k_j^{LTIP}(1-\alpha)LP_jC\left(\frac{CE_{LP_jC}}{CE_{LP_jC}+TG_{LP_jC}}\right)\left(\frac{TG_{CETP}}{CE_{CETP}+TG_{CETP}}\right)$$
$$\text{TG flux out of } LP_jC = \text{CE flux into } LP_jC$$
$$= 10^{-6}N_0k_{tr}k_j^{LTIP}(1-\alpha)LP_jC\left(\frac{TG_{LP_jC}}{CE_{LP_jC}+TG_{LP_jC}}\right)\left(\frac{CE_{CETP}}{CE_{CETP}+TG_{CETP}}\right) \quad (Eq.\ A9)$$

for j = 1,…,n.

These expressions are similar to the homoexchange rates in Eq. A7–A8, except that the (1−α) reflects the relative preference for heteroexchange. Note that in all four cases, the rates depend on the concentrations of the lipid leaving and entering the lipoprotein particle.

Combining the rates in Eq. A7–A9 with the binding kinetics as in Eq. A3, we have the following differential equations for the amount of CE and TG in LP_j bound to CETP:

$$\frac{dCE_{LP_jC}}{dt} = k_{on}V\left[CE_{LP_j^f}\right]\left[CETP^f\right] - k_{off}V\left[CE_{LP_jC}\right] + 10^{-6}N_0k_{tr}k_j^{LTIP}(1-\alpha)LP_jC(flux1-flux2) \quad (Eq.\ A10)$$

$$\frac{dTG_{LP_jC}}{dt} = k_{on}V\left[TG_{LP_j^f}\right]\left[CETP^f\right] - k_{off}V\left[TG_{LP_jC}\right] + 10^{-6}N_0k_{tr}k_j^{LTIP}(1-\alpha)LP_jC(flux2-flux1) \quad (Eq.\ A11)$$

for j = 1,…,n, where

$$flux1_j = \left(\frac{TG_{LP_jC}}{CE_{LP_jC}+TG_{LP_jC}}\right)\left(\frac{CE_{CETP}}{CE_{CETP}+TG_{CETP}}\right)$$
$$flux2_j = \left(\frac{CE_{LP_jC}}{CE_{LP_jC}+TG_{LP_jC}}\right)\left(\frac{TG_{CETP}}{CE_{CETP}+TG_{CETP}}\right) \quad (Eq.\ A12)$$

Note that the homoexchanges cancel out and do not explicitly appear in the differential equations because the exchange of two identical particles does not alter the composition of the lipoprotein. In the case of radiolabeled lipids, however, all four cases (*A*)–(*D*) must be included because there may be a homoexchange that involves both labeled and unlabeled lipid (e.g., radiolabeled CE exchanged with unlabeled CE).

The differential equations for the amounts of CE and TG associated with CETP include the transfer fluxes as in Eq. A10–A11:

$$\frac{dCE_{CETP}}{dt} = \sum_{j=1}^{n}10^{-6}N_0k_{tr}k_j^{LTIP}(1-\alpha)LP_jC(flux2_j - flux1_j) \quad (Eq.\ A13)$$

Downloaded from www.jlr.org by guest, on June 14, 2012

$$\frac{dTG_{CETP}}{dt}=\sum_{j=1}^{n}10^{-6}N_0k_{tr}k_j^{LTIP}(1-\alpha)LP_jC\left(flux1_j-flux2_j\right) \quad (Eq.\ A14)$$

where $flux1_j$ and $flux2_j$ are defined in Eq. A12.

The overall mathematical model then includes the six differential equations in Eq. A1, A3–A5, and A10–A11 for each lipoprotein species, together with the differential equations for unbound CETP (Eq. A2) and the lipids associated with CETP (Eq. A13–A14). Therefore, there are 6n+3 equations in the model.

The model can be augmented to include different mechanisms of CETP inhibition. For each inhibitor, at least one new species is added to the model. In the case of competitive inhibition, the concentration of unbound and CETP-bound inhibitor is included, with standard binding kinetics between inhibitor and CETP. An irreversible binding inhibitor would include the same species but there would be no dissociation of inhibitor-CETP complexes. Finally, a noncompetitive inhibitor would include these species plus the concentrations of inhibitor-CETP complex bound to each type of lipoprotein, with standard binding kinetics but no transfer activity.

Under equilibrium conditions, the rates of change of CETP binding and dissociation and of the CE and TG transfer activity are equal to zero, so that Eq. A1 implies that

$$k_{on}\left[LP_j^f\right]\left[CETP^f\right]=k_{off}\left[LP_jC\right] \quad (Eq.\ A15)$$

It follows from Eq. A15 and Eq. A10–A11 that flux1 = flux2, which further implies that

$$TG_{LP_jC}CE_{CETP}=CE_{LP_jC}TG_{CETP} \quad (Eq.\ A16)$$

Therefore, $CE_{CETP}/TG_{CETP}=CE_{LP_jC}/TG_{LP_jC}$ for j=1,…,n, so that at equilibrium, the CE:TG core lipid ratios of all lipoproteins are equal as in Assumption 8.

APPENDIX III: MODEL CALIBRATION

The model calibration process involves the sequential estimation of base and experiment-specific parameters according to the following heuristic algorithm:

1. Obtain an initial estimate of the base model parameters

a. Use all data sets

b. Do not vary the initial guess of the experiment-specific parameters

c. Estimate the base model parameters with least-squares optimization

2. Estimate unknown experiment-specific parameters

a. Use the base model parameters from Step 1, keeping them fixed

b. For each experiment, estimate the parameters specific only to that experiment using least-squares optimization

3. Reestimate all parameters simultaneously in a final optimization using all data sets

This approach is a pragmatic heuristic designed to minimize optimization problems and false convergences. The first two steps are designed to provide good starting estimates to Step 3. They simplify the problem to estimate either base model parameters or experiment-specific ones. Step 3 has no such restrictions, takes advantage of good starting estimates for the parameters (increasing optimization efficiency), reduces the likelihood of reaching a false minimum, and is designed to correct for any artifacts introduced in the prior steps. The optimizations were conducted using a standard pattern search technique (44). When available, error bars given with the experimental data (e.g., standard error of the mean) were utilized in the least squares optimization process as relative weights, so that data points with larger uncertainty carried less weight in the optimization than points with less uncertainty. When error bars were not provided with the data, a 10% standard error of the mean was assumed.

The authors gratefully thank Dr. Richard Morton of the Cleveland Clinic (Cleveland, OH) for his time and his insights into the biology of CETP. The authors also thank Dr. Mark Harpel of GlaxoSmithKline (King of Prussia, PA) for his insights into CETP inhibition mechanisms.

REFERENCES

1. Barter, P. J. 2002. Hugh Sinclair lecture: the regulation and remodelling of HDL by plasma factors. *Atheroscler. Suppl.* **3:** 39–47.
2. Yamashita, S., and Y. Matsuzawa. 1999. Cholesteryl ester transfer protein. *In* Lipoproteins in Health and Disease. D. J. Betteridge, D. R. Illingworth, and J. Shepherd, editors. Arnold, London. 277–299.
3. de Grooth, G. J., A. H. Klerkx, E. S. Stroes, A. F. Stalenhoef, J. J. Kastelein, and J. A. Kuivenhoven. 2004. A review of CETP and its relation to atherosclerosis. *J. Lipid Res.* **45:** 1967–1974.
4. Soutar, A. K. 1999. Low-density lipoprotein receptors. *In* Lipoproteins in Health and Disease. D. J. Betteridge, D. R. Illingworth, and J. Shepherd, editors. Arnold, London. 303–322.
5. Rader, D. J. 2003. Regulation of reverse cholesterol transport and clinical implications. *Am. J. Cardiol.* **92:** 42J–49J.
6. Barter, P. J., and J. J. Kastelein. 2006. Targeting cholesteryl ester transfer protein for the prevention and management of cardiovascular disease. *J. Am. Coll. Cardiol.* **47:** 492–499.
7. Athyros, V. G., D. P. Mikhailidis, A. I. Kakafika, A. Karagiannis, A. Hatzitolios, K. Tziomalos, E. S. Ganotakis, E. N. Liberopoulos, and M. Elisaf. 2007. Identifying and attaining LDL-C goals: mission accomplished? Next target: new therapeutic options to raise HDL-C levels. *Curr. Drug Targets.* **8:** 483–488.
8. Dullaart, R. P., G. M. Dallinga-Thie, B. H. Wolffenbuttel, and A. van Tol. 2007. CETP inhibition in cardiovascular risk management: a critical appraisal. *Eur. J. Clin. Invest.* **37:** 90–98.
9. Barter, P. J., M. Caulfield, M. Eriksson, S. M. Grundy, J. J. Kastelein, M. Komajda, J. Lopez-Sendon, L. Mosca, J. C. Tardif, D. D. Waters, et al. 2007. Effects of torcetrapib in patients at high risk for coronary events. *N Engl J Med.* **357:** 2109–2122.
10. Nicholls, S. J., D. M. Brennan, K. Wolski, S. R. Kalidindi, K.-W. Moon, E. M. Tuzcu, and S. E. Nissen. 2007. Abstract 684: Changes in levels of high density lipoprotein cholesterol predict the impact of torcetrapib on progression of coronary atherosclerosis: insights from ILLUSTRATE. *Circulation* **116:** II_127-b-.
11. Tall, A. R., L. Yvan-Charvet, and N. Wang. 2007. The failure of torcetrapib: was it the molecule or the mechanism? *Arterioscler. Thromb. Vasc. Biol.* **27:** 257–260.
12. Guerin, M., P. J. Dolphin, and M. J. Chapman. 1994. A new in vitro method for the simultaneous evaluation of cholesteryl ester ex-

Downloaded from www.jlr.org by guest, on June 14, 2012

change and mass transfer between HDL and apoB-containing lipoprotein subspecies. Identification of preferential cholesteryl ester acceptors in human plasma. *Arterioscler. Thromb.* **14:** 199–206.
13. Murakami, T., S. Michelagnoli, R. Longhi, G. Gianfranceschi, F. Pazzucconi, L. Calabresi, C. R. Sirtori, and G. Franceschini. 1995. Triglycerides are major determinants of cholesterol esterification/transfer and HDL remodeling in human plasma. *Arterioscler. Thromb. Vasc. Biol.* **15:** 1819–1828.
14. Le, N. A., W. Innis-Whitehouse, X. Li, R. Bakker-Arkema, D. Black, and W. V. Brown. 2000. Lipid and apolipoprotein levels and distribution in patients with hypertriglyceridemia: effect of triglyceride reductions with atorvastatin. *Metabolism.* **49:** 167–177.
15. Guerin, M., P. Egger, C. Soudant, W. Le Goff, A. van Tol, R. Dupuis, and M. J. Chapman. 2002. Cholesteryl ester flux from HDL to VLDL-1 is preferentially enhanced in type IIB hyperlipidemia in the postprandial state. *J. Lipid Res.* **43:** 1652–1660.
16. Guerin, M., W. Le Goff, T. S. Lassel, A. Van Tol, G. Steiner, and M. J. Chapman. 2001. Atherogenic role of elevated CE transfer from HDL to VLDL(1) and dense LDL in type 2 diabetes: impact of the degree of triglyceridemia. *Arterioscler. Thromb. Vasc. Biol.* **21:** 282–288.
17. Tall, A., D. Sammett, and E. Granot. 1986. Mechanisms of enhanced cholesteryl ester transfer from high density lipoproteins to apolipoprotein B-containing lipoproteins during alimentary lipemia. *J. Clin. Invest.* **77:** 1163–1172.
18. Lahdenpera, S., M. Syvanne, J. Kahri, and M. R. Taskinen. 1996. Regulation of low-density lipoprotein particle size distribution in NIDDM and coronary disease: importance of serum triglycerides. *Diabetologia.* **39:** 453–461.
19. Guerin, M., P. J. Dolphin, and M. J. Chapman. 1994. Preferential cholesteryl ester acceptors among the LDL subspecies of subjects with familial hypercholesterolemia. *Arterioscler. Thromb.* **14:** 679–685.
20. Barter, P., and K. A. Rye. 1994. Cholesteryl ester transfer protein: its role in plasma lipid transport. *Clin. Exp. Pharmacol. Physiol.* **21:** 663–672.
21. Tall, A. R. 1993. Plasma cholesteryl ester transfer protein. *J. Lipid Res.* **34:** 1255–1274.
22. Swenson, T. L., R. W. Brocia, and A. R. Tall. 1988. Plasma cholesteryl ester transfer protein has binding sites for neutral lipids and phospholipids. *J. Biol. Chem.* **263:** 5150–5157.
23. Ihm, J., D. M. Quinn, S. J. Busch, B. Chataing, and J. A. Harmony. 1982. Kinetics of plasma protein-catalyzed exchange of phosphatidylcholine and cholesteryl ester between plasma lipoproteins. *J. Lipid Res.* **23:** 1328–1341.
24. Qiu, X., A. Mistry, M. J. Ammirati, B. A. Chrunyk, R. W. Clark, Y. Cong, J. S. Culp, D. E. Danley, T. B. Freeman, K. F. Geoghegan, et al. 2007. Crystal structure of cholesteryl ester transfer protein reveals a long tunnel and four bound lipid molecules. *Nat. Struct. Mol. Biol.* **14:** 106–113.
25. Connolly, D. T., J. McIntyre, D. Heuvelman, E. E. Remsen, R. E. McKinnie, L. Vu, M. Melton, R. Monsell, E. S. Krul, and K. Glenn. 1996. Physical and kinetic characterization of recombinant human cholesteryl ester transfer protein. *Biochem. J.* **320:** 39–47.
26. Barter, P. J., G. J. Hopkins, L. Gorjatschko, and M. E. Jones. 1982. A unified model of esterified cholesterol exchanges between human plasma lipoproteins. *Atherosclerosis.* **44:** 27–40.
27. Barter, P. J., and M. E. Jones. 1980. Kinetic studies of the transfer of esterified cholesterol between human plasma low and high density lipoproteins. *J. Lipid Res.* **21:** 238–249.
28. Ko, K. W., T. Ohnishi, and S. Yokoyama. 1994. Triglyceride transfer is required for net cholesteryl ester transfer between lipoproteins in plasma by lipid transfer protein. Evidence for a hetero-exchange transfer mechanism demonstrated by using novel monoclonal antibodies. *J. Biol. Chem.* **269:** 28206–28213.
29. Morton, R. E., and D. J. Greene. 2003. The surface cholesteryl ester content of donor and acceptor particles regulates CETP: a liposome-based approach to assess the substrate properties of lipoproteins. *J. Lipid Res.* **44:** 1364–1372.
30. Morton, R. E., and D. B. Zilversmit. 1983. Inter-relationship of lipids transferred by the lipid-transfer protein isolated from human lipoprotein-deficient plasma. *J. Biol. Chem.* **258:** 11751–11757.
31. Serdyuk, A. P., and R. E. Morton. 1997. Lipid transfer inhibitor protein activity deficiency in normolipidemic uremic patients on continuous ambulatory peritoneal dialysis. *Arterioscler. Thromb. Vasc. Biol.* **17:** 1716–1724.
32. Barter, P. J., L. B. Chang, and O. V. Rajaram. 1990. Sodium oleate dissociates the heteroexchange of cholesteryl esters and triacylglycerol between HDL and triacylglycerol-rich lipoproteins. *Biochim. Biophys. Acta.* **1047:** 294–297.
33. Van Tol, A., L. M. Scheek, and J. E. Groener. 1991. Net mass transfer of cholesteryl esters from low density lipoproteins to high density lipoproteins in plasma from normolipidemic subjects. *Arterioscler. Thromb.* **11:** 55–63.
34. Barter, P. J., L. B. Chang, and O. V. Rajaram. 1990. Sodium oleate promotes a redistribution of cholesteryl esters from high to low density lipoproteins. *Atherosclerosis.* **84:** 13–24.
35. Liang, H. Q., K. A. Rye, and P. J. Barter. 1994. Dissociation of lipid-free apolipoprotein A-I from high density lipoproteins. *J. Lipid Res.* **35:** 1187–1199.
36. Serdyuk, A. P., and R. E. Morton. 1999. Lipid transfer inhibitor protein defines the participation of lipoproteins in lipid transfer reactions: CETP has no preference for cholesteryl esters in HDL versus LDL. *Arterioscler. Thromb. Vasc. Biol.* **19:** 718–726.
37. Deckelbaum, R. J., S. Eisenberg, Y. Oschry, E. Butbul, I. Sharon, and T. Olivecrona. 1982. Reversible modification of human plasma low density lipoproteins toward triglyceride-rich precursors. A mechanism for losing excess cholesterol esters. *J. Biol. Chem.* **257:** 6509–6517.
38. Shampine, L., and M. Reichelt. 1997. The MATLAB ODE Suite. *SIAM J. Sci. Comput.* **18:** 1–22.
39. Vogel, C. R. 2002. Computational methods for inverse problems. SIAM, Philadelphia.
40. Deckelbaum, R. J., S. Eisenberg, Y. Oschry, E. Granot, I. Sharon, and G. Bengtsson-Olivecrona. 1986. Conversion of human plasma high density lipoprotein-2 to high density lipoprotein-3. Roles of neutral lipid exchange and triglyceride lipases. *J. Biol. Chem.* **261:** 5201–5208.
41. Fukasawa, M., H. Arai, and K. Inoue. 1992. Establishment of anti-human cholesteryl ester transfer protein monoclonal antibodies and radioimmunoassaying of the level of cholesteryl ester transfer protein in human plasma. *J. Biochem.* **111:** 696–698.
42. Morton, R. E. 1985. Binding of plasma-derived lipid transfer protein to lipoprotein substrates. The role of binding in the lipid transfer process. *J. Biol. Chem.* **260:** 12593–12599.
43. Wang, X., D. M. Driscoll, and R. E. Morton. 1999. Molecular cloning and expression of lipid transfer inhibitor protein reveals its identity with apolipoprotein F. *J. Biol. Chem.* **274:** 1814–1820.
44. Lagarias, J. C., J. A. Reeds, M. H. Wright, and P. E. Wright. 1998. Convergence properties of the Nelder-Mead simplex method in low dimensions. *SIAM J. Optim.* **9:** 112–147.

Downloaded from www.jlr.org by guest, on June 14, 2012